Permafrost changes in the northwestern Da Xing'anling Mountains, Northeast China in the past decade

Xiaoli Chang [1,2★], Huijun Jin[2,3★], Ruixia He [2], Yanlin Zhang [1], Xiaoying Li [4], Xiaoying Jin [2] and Guoyu Li [2]

[1]School of Earth Science and Spatial Information Engineering, Hunan University of Science and Technology, Xiangtan, Hunan 411201, China,

[2]State Key Laboratory of Frozen Soils Engineering, Northwest Institute of Eco-Environment and Resources, Chinese Academy of Sciences, Lanzhou 730000, China,

[3]School of Civil Engineering, Institute of Cold-Regions Science and Engineering, and Northeast-China Observatory and Research-Station of Permafrost Geo-Environment (Ministry of Education), Northeast Forestry University, Harbin 150040, China,

[4]Key Laboratory of Sustainable Forest Ecosystem Management (Ministry of Education) and College of Forestry, Northeast Forestry University, Harbin 150040, China

★These authors contributed equally to this work.

Correspondence to: R. He: ruixiahe@lzb.ac.cn

Abstract. Under a pronounced climate warming, permafrost has been degrading in most areas globally, but it is still unclear in the northwestern part of the Da Xing'anling Mountains, Northeast China. According to a ten-year observation of permafrost and active-layer temperatures, the multi-year average of mean annual ground temperatures at 20 m was −2.83, −0.94, −0.80, −0.70, −0.60 and −0.49 °C, respectively, at Boreholes Gen'he4 (GH4), Mangui3 (MG3), Mangui1 (MG1), Mangui2 (MG2), Gen'he5 (GH5) and Yituli'he2 (YTLH2), with the depths of permafrost table varying from 1.1 to 7.0 m. Ground cooling at shallow depths has been detected, resulting in declining thaw depths in Yituli'he during 2009-2020, possibly due to relatively stable mean positive air temperature and declining snow cover and dwindling local population. In most study areas (e.g., Mangui and Gen'he), permafrost warming is particularly pronounced at larger depths (even at 80 m). These results can provide important information for regional development and engineering design and maintenance, and also provide a long-term ground temperature dataset for the validation of models relevant to the thermal dynamics of permafrost in the Da Xing'anling Mountains. All of the datasets are published through the National Tibetan Plateau Data Center (TPDC), and the link is https://doi.org/10.11888/Geocry.tpdc.271752 (Chang ~~X~~, 2021).

1 Introduction

Permafrost, defined as ground that remains at or below 0 °C consecutively for two or more years, is widespread in high-latitude and high-elevation regions (Zhang et al., 2007). One quarter of the Northern Hemisphere and 17% of the Earth's currently exposed land surface are underlain by permafrost (Gruber, 2012). ~~Areal extent of permafrost in China is estimated at about 1.59×10^6 km^2 (Youhua et al., 2012), mainly on the Qinghai-Tibet Plateau (about 1.06-1.17×10^6 km^2) (Zou et al., 2017; Cao et al., 2019), in northeastern China (about 3.1×10^5 km^2) (Zhang et al., 2021) and mountainous areas in northwestern China (Cao et al., 2018). Northern part of Northeast China is also characterized by the extensive and stable inversion of air temperature in winter, thick surficial deposits, dense vegetation, extensive snow cover, and widespread distribution of wetlands in valley bottoms and lowlands, resulting in strong regional differentiations in permafrost features (Jin et al., 2007). Therefore, the latitudinal permafrost in Northeast China is referred to as the "Xing'an (Hinggan)-Baikal permafrost (XBP)" (Jin et al., 2007), a distinct type of ecosystem-dominated permafrost (Shur and Jorgenson, 2007).~~

~~Permafrost is sensitive~~ Due to climate ~~change~~ warming (Farquharson et al., 2019; Sim et al., 2021; Zhang et al., 2019; Ran et al., 2018) and surface disturbances (Guo et al., 2018; Li et al., 2019; Li et al., 2021)~~.~~ ~~It, global~~ permafrost has experienced ~~significant warming and~~ widespread degradation during the last ~~several~~ decades (Jin et al., 2000; Jin et al., 2007; Zhang et al., 2019; Jin et al., 2021; Chen et al., 2020), evidenced by deeper seasonal thawing (Luo et al., 2018), thinning and warming permafrost (Gruber, 2012; Jin et al., 2021; Jin et al., 2007; Romanovsky et al., 2010; Wu et al., 2022) (Wu et al., 2022)~~{Wu, 2022 #2}~~, and ~~an~~ areal reduction ~~of permafrost in northeastern China~~ (Li et al., 2021; Zhang et al., 2021). ~~The p~~Permafrost change has attracted extensive attention worldwide (Biskaborn et al., 2019), because it has significant potential impacts on the terrestrial eco-hydrological processes (Zhang et al., 2017; Schuur and Mack, 2018; Zhang et al., 2018a; Ala-Aho et al., 2021; Ran et al., 2022; Luo et al., 2022) and carbon cycling (Mu et al., 2020; Schuur et al., 2015). In recent decades, huge efforts have been dedicated to developing physically based models aiming to reproduce and predict the thermal dynamic processes of permafrost and their consequences~~influences~~. However, lacking long term and systematic in-situ observation of permafrost temperature ~~is~~ becomes an apparent bottleneck for ~~the mentioned~~ relevant analysis and model calibration or validation. ~~The o~~Observations in deep ~~ground~~permafrost is especially rare and precious.

The areal extent of permafrost in China is estimated at about 1.59×10^6 km^2 (~~Youhua~~Ran et al., 2012), mainly in the mountainous areas of northwestern China (Cao et al., 2018), on the Qinghai-Tibet Plateau (about 1.06×10^6-1.17×10^6 km^2) (Zou et al., 2017; Cao et al., 2019), and in northeastern China (about 3.1×10^5 km^2) (Zhang et al., 2021). ~~As a main distribution region of high latitudes permafrost in China,~~ The northern part of Northeast China, e.g., the Da Xing'anling Mountains, is characterized by thick surficial deposit of organic soil and peat, dense vegetation, and widespread distribution of wetlands in valley bottoms and lowlands, and extensive and stable inversion of air temperature and snow cover in winter, resulting in strong regional differentiations in permafrost features (Jin et al., 2007). Therefore, the permafrost in the Da Xing'anling Mountains is referred to as "Xing'an (Hinggan)-Baikal permafrost (XBP)" (Jin et al., 2007), a distinct type of ecosystem-dominated permafrost (Shur and Jorgenson, 2007). However, the intensity and progress ~~on~~ of permafrost observation in ~~Da Xing'anling Mountains area~~ this region was falling far behind other permafrost regions in China, ~~.~~e.g., the Qinghai-Tibet~~an~~ Plateau (Zhao et al., 2021; Wu et al., 2022). Most ~~of~~ permafrost ~~such~~ investigation and observation in Da Xing'anling ~~mountains~~ Mountains ~~area~~ were aimed at serving some specific ~~short~~ short-term projects in economic development, engineering design and construction, e.g., road construction and coalmining (Jin et al., 2007), and they were terminated upon the project completion without persistence. In recent years, numerous local studies on permafrost change have been carried out. However, most of them ~~have been~~were based on air and/or ground surface temperatures provided by weather stations, reanalysis data (Wei et al., 2011; Zhang et al., 2018b; Zhang et al., 2021), or short-term ground thermal observations (He et al., 2021; Jin et al., 2007). ~~Thus~~Without direct observation of ground temperature profiles and their temporal changes, it is hard to more accurately feature and evaluate the latest distribution and future changes of permafrost in Northeast China under the combined influences of warming climate and human activities (Serban et al., 2021). Similar to the Circumpolar Active Layer Monitoring (CALM) sites (Brown et al., 2000; Grebenets et al., 2021; Shiklomanov et al., 2012), or CALM-South sites (Guglielmin, 2006; Guglielmin et al., 2012; Hrbáček et al., 2021), a comprehensive and persistent observing system was gradually established since 2009 at Gen'he (GH), Yituli'he (YTLH), and Mangui (MG) in the northwestern part of the Da Xing'anling Mountains, Northeast China. Periodical collection and calibration of data on the thermal regimes of soils in the active layer and permafrost at depths have been carried out in boreholes, generally reaching 20 m in depth and one of them, 80 m. Thus, ~~This~~ the observing system ~~thus~~ presents an opportunity to ~~observe~~ investigate the thermal characteristics of ~~the~~

XAP XBP at depths and to understand and evaluate the temporal changes in permafrost features in different landscapes under a warming climate. These data can provide important information for regional planning, development, and engineering design and maintenance in Northeast China. It can also provide data for long-term ground temperature datasets for the calibration and validation of models relevant to the thermal dynamics of permafrost in the Da Xing'anling Mountains., and provide important information for regional planning, development, and engineering design and maintenance in Northeast China.

2 Study area

The Gen'he Station of China Forest Ecological Research Network (CFERN), Yituli'he Permafrost Observatory (YPOYTLH), and Mangui Permafrost Station (MPSMG) are found in the discontinuous permafrost zone of Northeast China (Figure 1), where it is characterized by a cold temperate continental climate under the influences of alternating monsoons. The Multimulti-year averages of mean annual air temperature (MAAT) were was −4.0 °C at Gen'he (1961–2020), −5.2 °C at the YPOYituli'he (1965–2005), and −5.8 °C at the MPSMangui (1996–2005). In During the same periods, the multi-year average of annual precipitation was 440 mm at Gen'he, 460 mm at the Yituli'he YPO, and 480 mm at the MPSGangui (Yang, 2007). Annual The precipitation falls concentratively mainly in the form of summer rain, according to the meteorological records of Gen'he city, and Snowfall (snow water equivalent, SWE) accounts for about 12–20% (in snow water equivalent, SWE) of annual total precipitation. Stable snow cover on the ground surface usually starts to occur on the ground surface in the late October and generally disappears in the next April.

In the vicinity of CFERN, five boreholes were installed at Gen'he, and the datasets at GH4 and GH5 (Figure 1) with good quality were presented in this study. Two boreholes (YTLH1 and YTLH2) and three boreholes (MG1, MG2 and MG3) were installed at YTLH and MG, respectively (Figure 1). The Vvegetation differs slightly from site to site where at all mentioned Boreholes GH4, GH5, YTLH1, YTLH2, MG1, MG2 and MG3 are located (Figure 1 and Table 1). Borehole For example, GH4 is located in a larch (*Larix gmelinii*) forest, whereas Boreholes GH5, YTLH1, YTLH2 and MG2 are in sedge (*Carex tato*) meadows. The Borehole MG3 is in an open backyard, and Borehole MG1, is located in a birch (*Betula*) shrubland with sedges (*Carex tato*) as an understory. However, The soil types at all boreholes are similar the same, i.e., (brown coniferous forest soil).

Among the seven boreholes, Borehole YTLH1 of with a depth of 8.15 m in depth was first installed for monitoring the hydrothermal dynamics of active layer and shallow permafrost at the end of 2008, with weekly manual measurement of soil temperatures since 2009. However, in order to monitor the permafrost temperature at the depth of zero annual amplitude (generally at 10-25 m in Northeast China), a depth of 20 m at a nearby site (10 m away from the YTLH1) with almost identical physical and vegetative conditions on the ground surface. ~~The t~~Thermistor cables for monitoring the ground temperatures were permanently installed in the boreholes ~~for manually monitoring ground temperatures~~ since 2010. ~~Boreholes~~ GH4, GH5, MG1, MG2 and MG3 have been ~~monitored~~ installed and started working since the beginning of 2012, but ~~for~~ with different observational frequencies (Table 1). ~~These~~ All the thermistor cables were assembled with same technology standards by the State Key Laboratory of Frozen Soils Engineering (SKLFSE~~),~~) in Cold and Arid Regions Environmental and Engineering Research Institute (CAREERI; now renamed to the Northwest Institute of Eco-Environment and Resources, or NIEER~~),~~) of CAS ~~Chinese Academy of Sciences~~ (Chinese Academy of Sciences ~~CAS~~)~~, Lanzhou, China~~. The ~~, with an~~ accuracy of ground temperature measurement is ±0.05 °C in the temperature range from −30 to +30 °C, and ±0.1 °C~~,~~ in ranges from −45 to −30 °C and from +30 to +50°C.

Among the seven boreholes, ~~Borehole~~ YTLH1 ~~of~~ with a depth of 8.15 m ~~in depth~~ was first installed for monitoring the hydrothermal dynamics of active layer and shallow permafrost at the end of 2008, with weekly manual measurement of soil temperatures since 2009. However, in order to monitor the permafrost temperature at the depth of zero annual amplitude (generally at 10-25 m in Northeast China), ~~an additional borehole (~~YTLH2~~)~~ was drilled to a depth of 20 m at a nearby site (10 m away from the YTLH1) with almost identical physical and vegetative conditions on the ground surface. ~~The t~~Thermistor cables for monitoring the ground temperatures were permanently installed in the boreholes ~~for manually monitoring ground temperatures~~ since 2010. ~~Boreholes~~ GH4, GH5, MG1, MG2 and MG3 have been ~~monitored~~ installed and started working since the beginning of 2012, but ~~for~~ with different observational frequencies (Table 1). ~~These~~ All the thermistor cables were assembled with same technology standards by the State Key Laboratory of Frozen Soils Engineering (SKLFSE~~),~~) in Cold and Arid Regions Environmental and Engineering Research Institute (CAREERI; now renamed to the Northwest Institute of Eco-Environment and Resources, or NIEER~~),~~) of CAS ~~Chinese Academy of Sciences~~ (Chinese Academy of Sciences ~~CAS~~)~~, Lanzhou, China~~. The ~~, with an~~ accuracy of ground temperature measurement is ±0.05 °C in the temperature range from −30 to +30 °C, and ±0.1 °C~~,~~ in ranges from −45 to −30 °C and from +30 to +50°C.

For continuous observation, the thermistor cables at GH4 were connected to ~~data fora~~ a Micrologger of CR3000 (USA), and the ground temperatures ~~at the Borehole GH4~~ were automatically collected in an hourly ~~by~~time step~~ the Micrologger CR3000 (USA)~~, whereas the ground temperatures at other ~~sites~~ boreholes were manually measured with a multi-meter (Fluke 189®). Unfortunately, not all records for ~~soil~~ ground temperatures are complete in time for all boreholes. For example, there were two hiatuses for the records of ~~Borehole~~ GH4 (2014-2016 and 2017-2019) due to the logger damage. Manual records from January to June in 2014 for other boreholes were lost in mailing. The measurement at MG3 was halted in 2016 because of borehole damage and that at GH5 and YTLH2, in 2020, due to the outbreak of the COVID-19 virus and the ensued traffic control. The specifics are presented in Table 1.

3 Results

3.1 Ground temperatures in near-surface permafrost and active layer

Ground temperatures of near-surface soil (e.g., at depths of 1 and 2 m) responds quickly to changes in air temperature, but the change patterns of ground temperatures show a reduction of amplitude with increasing depth in all ~~these~~ boreholes. In ~~Boreholes~~ boreholes GH4, MG3, YTLH1 and YTLH2, seasonal variations in ground temperature still could be detected at the depth of 5 m. However, at depths of 3 and 4 m, variations in winter ground temperatures gradually flattens out in ~~Boreholes~~ boreholes GH5, MG1 and MG2, and only the annual variability in summer ground temperatures can be detected at the depth of 5 m (Figure 2). Therefore, only a small temperature amplitude (0.5~1.0°C) was detected at the depth of 5 m in comparison with that at 3 m (2~3°C).

Based on the thermal observation at ~~Borehole~~ MG1, 2.6 m (2017) and 1.9 m (2020) in depth were respectively the maximum and minimum depths of ~~the~~ permafrost table (Table 2). Combining the data in Figure 2b and other observational data, the active layer thickness (ALT) at ~~Borehole~~ MG2 increased from 4.3 m (2012) to 4.8 m (2016), but thinned to 4.2 m (2019) afterwards. The permafrost table at MG3 was located at 2.8 m (2012 and 2013), 4.0 m (2014) and 3.3 m (2015) in depth during the observation period. Subtle freeze-thaw cycles were observed at 2.0 m in depth in ~~Borehole~~ GH4 (Figure $2a_2$), and the 0 °C isotherms in Figure 3a indicated a range of ALT from 2.2 m (2016) to 2.0 m (2018). In ~~Borehole~~ GH5, there still exist obvious freeze-thaw cycles at the depth of 6.0 m, despite ~~of~~ with a small varying range in ground temperature ~~range~~ (0.5°C)~~ at the depth of 6.0 m, freeze-thaw cycles took place~~. ~~During the monitoring period,~~ However, the ~~sensor~~ ground temperature at the depth of 7.0 m stayed constantly below 0 °C all year round during the monitoring period~~in depth showed all negative temperatures~~, ~~ap~~but

~~in the left~~ proxim~~ity~~ating ~~of~~ to 0 °C and~~,~~ ~~all year round,~~ with a multi-year average of mean annual ~~soil~~ ground temperature at –0.08°C. That is, ~~T~~the thawing front reached down to the depth of 7.0 m every year (Figure 3b), which means the permafrost table here has been lowered to 7.0 m in depth. In ~~Borehole~~ YTLH1, ground thawing occurred occasionally at 2.0 m, for an example, in October 2016, but the ALT mostly varied from 1.5 m (2011) to 1.0 m (2017) during the observation (Figure 3c). In the same period in 2016, –0.1 °C was registered as the highest temperature at 2.0 m in depth in ~~Borehole~~ YTLH2 (Figure 2c_2), but an above-zero temperature~~,~~ at 1.5 m depth. The depth of ~~the~~ permafrost table fluctuated between 1.6 m (2017) and 2.0 m (2011 and 2016) (Figure 3d and Table 2).

3.2 Changes ~~trends~~ of permafrost temperature at depth~~s~~

Figure 4 highlights the changes in thermal regimes of permafrost at different depths in ~~Boreholes~~ boreholes MG1, MG2 and MG3. Ground temperature was on the rise, but its amplitude decreased with depth since the beginning of observation in 2012. The depth of zero annual amplitude (ZAA) was estimated to be the place where ground temperature changes by no more than 0.1°C throughout a year (Everdingen, 1998 (revised 2005)). Although the ground temperature was not measured periodically with a very fine time step and some values were lost, the estimation could still be reasonable, because the temperature fluctuation in deep ground is significantly dampened. According to the monitoring data, the depth of ZAA varies among different boreholes (Table 2) without considering interannual changes. In order to show more accurate thermal statses of permafrost, ground termperatures of 20 m were chosen to compare within different boreholes in this ~~paper~~study. In ~~Borehole~~ MG1, the varying amplitudes of ground temperatures for depths deeper than~~below~~ 8 m ~~in depth was~~were no more than 0.4 °C, and seasonal variability was hardly detectable at depths of 16 and 20 m. The results of linear fitting (red trend lines) indicate an overall warming trend of permafrost during 2012-2020. A mulit-year average of mean annual ground temperature (MAGT, at 20 m; from 2012 to 2020) of –0.77 °C was obtained in ~~Borehole~~ borehole MG1. In ~~Borehole~~ MG2, the ground temperature varied slightly (±0.06°C) with the seasons even at the depth of 20 m, where the MAGT was about –0.69 °C. Permafrost here was also warming, with a rising amplitude of 0.1~0.2 °C from 2012 to 2020. The valid monitoring period was less than 5 years in ~~Borehole~~ MG3 (1 January 2012 to 29 April 2016), when the largest ground temperature range of 0.2-0.5 °C was detected between the depths from 8 ~~m and~~ to 20 m. Similar to ~~the Borehole~~ that in MG2, the pemafrost temperature at the depth of 20 m ~~in depth~~ in ~~Borehole~~ borehole MG3 has been experiencing some seasonal variations, with a multi-year average of MAGT at –0.94 °C (Table 2). During 2012-2020, ~~Permafrost~~ permafrost at depths of 8 and 20 m in ~~Boreholes~~ GH4 and GH5 (Figure 5) warmed by 1.5-0.2 and 0.2-0.1°C, respectively~~, during 2012-2020~~. The warming of permafrost at GH5 was insignificant in comparison with that at other sites. Mean annual ~~soil~~ ground temperature at 8 m in depth have slightly warmed from –0.17 °C in 2012 to –0.16 °C in 2019, and; the MAGT at 20 m in depth, from –0.60 to –0.57 °C over the same period. MAGT at 20 m in depth was averaged at –0.59 °C during 2012-2019. However, permafrost at GH4 was ~~relatively~~ obviously colder, with a multi-year average of MAGT at –2.84 °C at 20 m in depth. According to Figure 5, ground temperatures fluctuated seasonally at depths of 8-~~above~~ 20 m~~ in depth~~. However, seasonal variations in ground temperature dwindled gradually ~~below~~ at depths deeper than 30 m (Figure 6), leaving only inter-annual variations. Ground temperatures in ~~Borehole~~ GH4 increased with increasing depth (–2.51, –1.76 and –0.41 °C at 30, 50 and 80 m, respectively), whereas the thermal fluctuations declined downwards (0.2 °C at 20 and 30 m in depth, but 0.03 °C at 80 m). ~~Thus, d~~During 2012-2020, the ~~ground~~ permafrost at depths of 30-80 m at ~~the~~ GH4 ~~site~~ was warming at an average rate of 0.04-0.20 °C /dec.

In Borehole YTLH2, remarkable seasonal variations were noted at each measured depth. The seasonal amplitude of ground temperature gradually dampened with increasing depth, varying from approximately 0.5 °C at 8 m in depth to less than 0.1 °C at 20 m. Unlike permafrost in Mangui town and Gen'he city, a significant cooling of permafrost was detected at all depths except 20 m at YTLH2 during the 10-year observation (Figure 7). The average rate of temperature change at 20 m depth is close to 0 °C /dec and the MAGT here has been roughly maintained at –0.49 °C in the past decade (Table 2).

4 Discussion

4.1 Changes ~~trends~~ of near-surface permafrost temperatures

Based on the analysis in Section 3.1, it can be inferred that changes in ~~the~~ ground thermal regimes (especially in ALT) of the ecosystem-dominated permafrost on the northwestern slope of ~~the~~ Da Xing'anling Mountains are mainly controlled by the changes in local factors, such as vegetation and snow covers and human activities~~, especially in the ALT~~. For example, ALT ranges from 2.5 m in 2016 and 2017 to 1.9 m in 2020 for the ~~site~~ borehole in shrubs (MG1), 4.8 m in 2017 to 4.2 m in 2020 for the borehole in sedge meadow (MG2), and 2.9 m in 2012 to 4.0 m in 2014 for the borehole in ~~the~~ a farmer's backyard (MG3) during the observation period. Apparently, the ~~Borehole~~ borehole MG1, far away from downtown Mangui, had the least ALT because of more shading effect of shrubs than that of meadow (MG2) and less anthropogenic impact than that of backyard (MG3). A ~~D~~declining trend of ALT was also observed in the Nanwenghe Wetlands Reserve on the southern slope of the Da Xing'aning-Yile'huli Mountain Knots, Northeast China, probably driven by a rising surface and thermal offsets of vegetation cover and organic soils (He et al., 2021). Additionally, at ~~the~~ MG3 ~~site~~, the smaller ALT could be attributed to the shading effect of the farmer's house and more heat loss to the atmosphere caused by snow removal in the yard in winter as well. In Gen'he, at the site of ~~Borehole~~ GH4 in a primeval forest, ALT remained unchanged at 2.2 m from 2012 to 2016 and, without human disturbance, permafrost was well-preserved. On the contrary, at the GH5 site in the suburb meadow frequently disturbed by the nearby livestock, a complex thermal regime was observed in the active layer. Ground temperatures at the depths of 3.5-6.0 m were ~~negative~~ below 0^{o} C from March to September and above 0^{o} C ~~positive~~ in other time every year, and; not until 7.0 m in depth, where it became below 0^{o} C all the year round. By definition, the active layer is the layer above permafrost that freezes in winter and thaws in summer. Therefore, 7 m is supposed to be the reasonable ALT or the depth of ~~the~~ permafrost table, and there might be no supra-permafrost subaerial talik (Jin et al., 2021) between the active layer and the permafrost table at this site, i.e., attached permafrost. However, the supra-permafrost subaerial talik, which has appeared in the Nanwenghe Wetlands Reserve about 300 km to the east of the study site (He et al., 2021), may develop at this site in ~~the~~ future. In Yituli'he, the two boreholes (YTLH1 and YTLH2) are, about 20 m apart, both in the meadowy swamp to the east of the railway and to the west of highway. Permafrost here is well developed, partially ~~thanks~~attributed to the sufficient moisture provided by lowland swamp, which also possibly facilitates the formation of ice wedges (Yang and Jin, 2011).

Notably, there was a decreasing trend in ground temperatures at shallow depths no matter in summer or winter during 2010-2020 (Figure 2), ~~otherwise~~ suggesting a cooling permafrost at shallow depths in the last decade on the northwestern slope of the Da Xing'anling Mountains ~~if no ground-surface conditions are taken into account~~. The maximum thaw depth (MTD) in Yituli'he rose gradually with fluctuations during 1980-2005, and it showed a downward trend during 2010-2019 (Figure 8). This could be related to the thriving vegetation, and declining winter precipitation or snow cover in this area during the observational period. In the last decade, although the mean positive air temperature (MPAT) barely changed in Gen'he (Fig 9b), precipitation in warm seasons increased slightly, leading to a wetter condition in favor of vegetation thriving. For example, the maximum vegetation height of *Carex tato* at YTLH1 and YTLH2 grew significantly from 2009 to 2014. Bushes have also emerged recently near the borehole. Thriving vegetation ~~will~~ reduces the solar irradiance incident onto the soil surface in summer, ~~and cast a~~ cooling ~~effect on~~ the ground ~~temperature~~. On the contrary, the winter precipitation (Figure 9a) and snow cover, including the maximal snow depth (Figure 9c) and snow duration (Figure 9d), declined slightly. The thermal insulation effect of snow cover ~~will be weakened~~ weakens when ~~the snow~~ the depth of snow cover ~~decreased~~declines, which will lead to a larger heat removal from the permafrost to air in winter and drive the permafrost cooling. ~~The d~~Detailed mechanisms for the cooling permafrost will be further investigated with the help of some physically based models after complementing observations on the interactions of energy balance between the permafrost, vegetation, and snow cover.

4.2 Changes ~~trends~~ of permafrost temperatures at ~~larger~~ depth~~s~~

Permafrost in Mangui

During the observation period, the averages of MAGTs at the depth of 20 m were –0.79, –0.70 and –0.93 °C, respectively, in shrubs (MG1), meadow (MG2) and the farmer's backyard (MG3), indicating a poor correlation between the thermal state of deep~~er~~ permafrost and vegetation cover or anthropic disturbances. However, there was a close relationship between the permafrost change at ~~larger~~ depth~~s~~ and land surface conditions. The ~~P~~permafrost ~~below~~ deeper than 8 m was significantly warming in the last decade under a warming climate (Figure 4). In ~~Borehole~~ MG1 and ~~Borehole~~ MG2 in particular, the rates of ground warming increased slightly with depth (<0.3 °C/dec for MG1 and <0.2 °C/dec for MG2)~~, demonstrating a less significant thermal rising in deeper permafrost~~. Within the zone of discontinuous permafrost, the negative relationship between effective leaf area index (LAI_e) and soil moisture content may contribute to differential rates of permafrost thaw (Baltzer et al., 2014). Therefore, more effective water uptake by shrubs than meadow results in lower soil moisture, leading to a more rapid thaw of permafrost at ~~the~~ MG1 ~~site~~ than that at ~~the~~ MG2 ~~site~~. The warming rate of permafrost in ~~Borehole~~ MG3, with a large warming range, decreased with depth (0.5 °C/dec at depths of 10 and 12 m, but approximately 0.2 °C/dec at depths of 16 and 20 m), probably due to short monitoring period and less data. However, it does verify that, in Mangui, permafrost at depth~~s~~ is warming or degrading in the last decade.

Permafrost in Gen'he

Indeed, there exists some long periods with missing data at GH4~~, and it is reluctant to make the trend~~

~~analysis with these missing data~~. However, ~~at the surface layers,~~ although the fluctuation of ground temperatures is relatively ~~huge~~ large at surface layers, the collected data ~~has~~ have generally captured the maximal and minimal ground temperature ~~in~~ for some important years ~~with observing data~~. Simply by a visual inspection, the minimal or maximal ground temperatures in the observed years has an apparent warming trend from 2012 to 2020, which has a good coincidence with the trend analysis in this study. That is, although the missing values could make some loss for the accuracy of trending analysis, or make it less robust, they will not change the trend in an antipodal way. In addition, in ~~depths~~ the ground ~~greater~~ deeper than 8 m, the annual fluctuation of ground temperature was much less than that in the surface layers, as shown in Figures 5 and 6. The missing values will not vary too much from the closest collected values in time. Therefore, we ~~speculate~~ assume that the influence of missing values on the trending analysis ~~for~~ of ground temperature at depth~~deep layers~~ will be smaller than that in the surface layers, and it will decrease with depth, which can be inferred from Figures 5 and 6.

In ~~Borehole~~ GH4, lower ground temperatures and greater warming ~~range~~ rates ~~was~~ were observed in comparison with those in ~~Borehole~~ GH5 in the last decade (Figure 5). Even at the depths of 70 and 80 m, the ground temperatures were still rising with time at appreciable warming rates (Figure 6)~~, reflecting the impact of climatic warming on permafrost at greater depths~~. A subtle warming trend of permafrost at depths of 8-20 m in ~~Borehole~~ GH5 was also detected with a rate of 0.04 ℃/dec during the observation period (Figure 5). This warming rate of ground temperature is similar to that of the Borehole 85-8A in the southern zone of discontinuous permafrost in North America, where the permafrost is often vertically in isothermal condition and close to 0 ℃ in ground temperature (Smith et al., 2010). In this situation, latent heat effects are considered as the key factor for leading to isothermal conditions in the ground and allowing permafrost to persist under a warming climate (Smith et al., 2010). If the effect of large thermal inertia lasts long enough, the supra-permafrost subaerial talik will be highly likely to form and permafrost will be gradually buried. ~~In a word~~Overall, the permafrost at depth in forested landscape ~~degradation~~ in Gen'he is ~~also~~ taking an evident and ongoing warming trend at present~~ in both forested landscape and anthropic zones, particularly in the latter one~~.

Permafrost in Yituli'he

According to a previous study (Jin et al., 2007), MAGT at 13 m in Yituli'he rose by 0.2 ℃ during 1984-1997, continuously rising from –1.00 ℃ in 1997 to –0.55 ℃ in 2010, except during the short suspension of monitoring (2005-2008), and peaking at –0.53 °C in 2013. After that, it kept lowering consecutively and by 2018 it was lower than –0.70 °C, showing an evident cooling trend of permafrost in a sharp contrast to the ground warming trends in Gen’he, Mangui, and other permafrost regions in the world (Douglas et al., 2021; Farquharson et al., 2019). Based on ~~the~~ an investigation, there was once a Railway Branch Administration in Yituli’he town since 1964s to 1970s, with a population of over 30,000, but the branch was terminated in 1998. After that, more and more people emigrated and less than 10,000 residents have remained at present, thus leaving a chance for ~~restoration~~ recovery of the local eco-environment and ~~for recovering~~ permafrost temperature.

So far, the mitigation of permafrost degradation becomes considerably difficult in the context of a persistent climate warming (Brown et al., 2015; Luo et al., 2018). However, within the dried margin of the Twelvemile Lake (66°27′N, 145°34′W), permafrost aggradation has taken place due to willow shrub uptake of summer recharge and summer shading recharge reduction (Briggs et al., 2014). Beer et al. (Beer et al., 2020) also found that most permafrost-affected soil could be preserved by increasing the population density of big herbivores in northern high-latitude ecosystems as a result of reducing insulation of winter snow cover. The fact that permafrost is cooling in Yituli’he demonstrates that the ecosystem-protected permafrost in discontinuous permafrost zone may recover if the disturbances, such as human activities, dwindle. Thus, our research results would provide key evidence for the preservation of permafrost in areas with intense past anthropic disturbances (Serban et al., 2021).

5 Conclusions

Long-term records of permafrost monitoring presented here from the northwestern flank of the Da Xing’anling Mountains in Northeast China show some important characteristics of ground thermal regimes in the past eight years (2012-2020). The lowest MAGT at 20 m in depth was –2.83 °C in ~~Borehole~~ GH4 in a primeval larch forest, and –0.94, –0.80, –0.70, –0.60 and –0.49 °C, respectively, at MG3, MG1, MG2, GH5 and YTLH2. The maximum of ~~the~~ burial depth of ~~the~~ permafrost table at about 7.0 m was discovered in ~~Borehole~~ GH5, and the minimum, 1.1 ~ 1.5 m at YTLH1. The permafrost table was at depths of about 2.0 m at GH4 and YTLH2, and 2.5, 5.0 and 4.0 m at MG1, MG2 and MG3, respectively. Local factors, such as vegetation and snow covers and human activities, are supposed to be mainly responsible for the changes in ~~the~~ ALT and ~~the~~ thermal state of shallow permafrost in the study area. The most important fact is that ground cooling at shallow depths, as well as the declining ALT in Yituli'he after 2009, has been detected during the observation period, which is probably caused by fairly constant MPAT (mean positive air temperature) and weakened insulation of winter snow cover.

Apart from Yituli'he, permafrost warming at ~~large depths~~depth was particularly pronounced during the observation period, even at depths of 70 and 80 m, with different ground warming rates. It is noteworthy that the geothermal gradient at depth~~s~~ in ~~Borehole~~ GH5 is almost zero (vertically no change) and with MAGT at about 0 °C due to huge thermal inertia of the ice-rich permafrost. This may most likely lead to the formation of ~~the~~ supra-permafrost subaerial talik soon. At the Yituli'he Permafrost Observatory, permafrost has been cooling since the re-establishment of monitoring program in 2010; the rapidly declining local population might have relieved its stress on the eco-environment and resulted in permafrost recovery. This fact makes it possible to mitigate the permafrost degradation in ~~the~~ zones of ecosystem-dominated permafrost, offering a new thought for permafrost protection.

Author Contributions

XC, HJ, and RH designed the study. XC wrote the manuscript and performed the analysis. YZ plotted the figures. XL, XJ and GL contributed parts of the field data. HJ improved the writing and structure of the paper.

Competing interests

The contact author has declared that neither they nor their co-authors have any competing interests.

Disclaimer

Publisher's note: Copernicus Publications remains neutral with regard to jurisdictional claims in published maps and institutional affiliations.

Special issue statement

This article is part of the special issue "Extreme ~~environment~~ Environment ~~datasets~~ Datasets for the ~~three~~ Three ~~p~~Poles". It is not associated with a conference.

Acknowledgements

Thanks go to the Inner Mongolia Agricultural University for fieldwork support and the Gen'he Weather Bureau for meteorological data provision. This study was financially supported by the National Natural

Science Foundation of China (Grant Nos. 41971079, 41671059, 41871052 and U20A2082) and the Natural Science Program of Hunan Province (Grant No. 2020JJ5161).

Data availability

The dataset is available from the National Tibetan Plateau/Third Pole Environment Data Center (https://doi.org/10.11888/Geocry.tpdc.271752, Chang X, 2021).

Reference

Ala-Aho, P., Autio, A., Bhattacharjee, J., Isokangas, E., Kujala, K., Marttila, H., Menberu, M., Meriö, L. J., Postila, H., Rauhala, A., Ronkanen, A. K., Rossi, P. M., Saari, M., Haghighi, A. T., and Kløve, B.: What conditions favor the influence of seasonally frozen ground on hydrological partitioning? A systematic review, Environmental Research Letters, 16, 043008, 10.1088/1748-9326/abe82c, 2021.

Baltzer, J. L., Veness, T., Chasmer, L. E., Sniderhan, A. E., and Quinton, W. L.: Forests on thawing permafrost: fragmentation, edge effects, and net forest loss, Global change biology, 20, 824-834, 10.1111/gcb.12349, 2014.

Beer, C., Zimov, N., Olofsson, J., Porada, P., and Zimov, S.: Protection of Permafrost Soils from Thawing by Increasing Herbivore Density, Scientific reports, 10, 4170, 10.1038/s41598-020-60938-y, 2020.

Biskaborn, B. K., Smith, S. L., Noetzli, J., Matthes, H., Vieira, G., Streletskiy, D. A., Schoeneich, P., Romanovsky, V. E., Lewkowicz, A. G., Abramov, A., Allard, M., Boike, J., Cable, W. L., Christiansen, H. H., Delaloye, R., Diekmann, B., Drozdov, D., Etzelmüller, B., Grosse, G., Guglielmin, M., Ingeman-Nielsen, T., Isaksen, K., Ishikawa, M., Johansson, M., Johannsson, H., Joo, A., Kaverin, D., Kholodov, A., Konstantinov, P., Kröger, T., Lambiel, C., Lanckman, J.-P., Luo, D., Malkova, G., Meiklejohn, I., Moskalenko, N., Oliva, M., Phillips, M., Ramos, M., Sannel, A. B. K., Sergeev, D., Seybold, C., Skryabin, P., Vasiliev, A., Wu, Q., Yoshikawa, K., Zheleznyak, M., and Lantuit, H.: Permafrost is warming at a global scale, Nature Communications, 10, 264, 10.1038/s41467-018-08240-4, 2019.

Briggs, M. A., Walvoord, M. A., McKenzie, J. M., Voss, C. I., Day-Lewis, F. D., and Lane, J. W.: New permafrost is forming around shrinking Arctic lakes, but will it last?, Geophysical Research Letters, 41, 1585-1592, https://doi.org/10.1002/2014GL059251, 2014.

Brown, D. R. N., Jorgenson, M. T., Douglas, T. A., Romanovsky, V. E., Kielland, K., Hiemstra, C., Euskirchen, E. S., and Ruess, R. W.: Interactive effects of wildfire and climate on permafrost degradation in Alaskan lowland forests, Journal of Geophysical Research: Biogeosciences, 120, 1619-1637, https://doi.org/10.1002/2015JG003033, 2015.

Brown, J., Hinkel, K. M., and Nelson, F. E.: The circumpolar active layer monitoring (calm) program: Research designs and initial results, Polar Geography, 24, 166-258, 10.1080/10889370009377698, 2000.

Cao, B., Zhang, T., Wu, Q., Sheng, Y., Zhao, L., and Zou, D.: Permafrost zonation index map and statistics over the Qinghai-Tibet Plateau based on field evidence, Permafrost and Periglacial Processes, 30, 178-194, 10.1002/ppp.2006, 2019.

Cao, B., Zhang, T., Peng, X., Mu, C., Wang, Q., Zheng, L., Wang, K., and Zhong, X.: Thermal Characteristics and Recent Changes of Permafrost in the Upper Reaches of the Heihe River Basin, Western China, Journal of Geophysical Research: Atmospheres, 123, 7935-7949, https://doi.org/10.1029/2018JD028442, 2018.

Chen, S.-S., Zang, S., and Sun, L.: Characteristics of permafrost degradation in Northeast China and its ecological effects: A review, Sciences in Cold and Arid Regions, 12, 1-11, 10.3724/sp.j.1226.2020.00001., 2020.

Douglas, T. A., Hiemstra, C. A., Anderson, J. E., Barbato, R. A., Bjella, K. L., Deeb, E. J., Gelvin, A. B., Nelsen, P. E., Newman, S. D., Saari, S. P., and Wagner, A. M.: Recent degradation of interior Alaska permafrost mapped with ground surveys, geophysics, deep drilling, and repeat airborne lidar, The Cryosphere, 15, 3555-3575, 10.5194/tc-15-3555-2021, 2021.

Everdingen, R. O. v.: Multi-language glossary of permafrost and related ground-ice terms, National Snow and Ice Data Centre, Boulder, CO1998 (revised 2005).

Farquharson, L. M., Romanovsky, V. E., Cable, W. L., Walker, D. A., Kokelj, S. V., and Nicolsky, D.: Climate Change Drives Widespread and Rapid Thermokarst Development in Very Cold Permafrost in the Canadian High Arctic, Geophysical Research Letters, 46, 6681-6689, https://doi.org/10.1029/2019GL082187, 2019.

Grebenets, V. I., Tolmanov, V. A., and Streletskiy, D. A.: Active Layer Dynamics Near Norilsk, Taimyr Peninsula, Russia, Geography, Environment, Sustainability, 14, 55-66, 10.24057/2071-9388-2021-073, 2021.

Gruber, S.: Derivation and analysis of a high-resolution estimate of global permafrost zonation, The Cryosphere, 6, 10.5194/tc-6-221-2012, 2012.

Guglielmin, M.: Ground surface temperature (GST), active layer and permafrost monitoring in continental Antarctica, Permafrost and Periglacial Processes, 17, 133-143, https://doi.org/10.1002/ppp.553, 2006.

Guglielmin, M., Worland, M. R., and Cannone, N.: Spatial and temporal variability of ground surface temperature and active layer thickness at the margin of maritime Antarctica, Signy Island, Geomorphology, 155-156, 20-33, https://doi.org/10.1016/j.geomorph.2011.12.016, 2012.

Guo, W., Liu, H., Anenkhonov, O. A., Shangguan, H., Sandanov, D. V., Korolyuk, A. Y., Hu, G., and Wu, X.: Vegetation can strongly regulate permafrost degradation at its southern edge through changing surface freeze-thaw processes, Agricultural and Forest Meteorology, 252, 10-17, https://doi.org/10.1016/j.agrformet.2018.01.010, 2018.

He, R.-X., Jin, H.-J., Luo, D.-L., Li, X.-Y., Zhou, C.-F., Jia, N., Jin, X.-Y., Li, X.-Y., Che, T., Yang, X., Wang, L.-Z., Li, W.-H., Wei, C.-L., Chang, X.-L., and Yu, S.-P.: Permafrost changes in the Nanwenghe Wetlands Reserve on the southern slope of the Da Xing'anling–Yile'huli mountains, Northeast China, Advances in Climate Change Research, 12, 696-709, https://doi.org/10.1016/j.accre.2021.06.007, 2021.

Hrbáček, F., Vieira, G., Oliva, M., Balks, M., Guglielmin, M., de Pablo, M. Á., Molina, A., Ramos, M., Goyanes, G., Meiklejohn, I., Abramov, A., Demidov, N., Fedorov-Davydov, D., Lupachev, A., Rivkina, E., Láska, K., Kňažková, M., Nývlt, D., Raffi, R., Strelin, J., Sone, T., Fukui, K., Dolgikh, A., Zazovskaya, E., Mergelov, N., Osokin, N., and Miamin, V.: Active layer monitoring in Antarctica: an overview of results from 2006 to 2015, Polar Geography, 44, 217-231, 10.1080/1088937X.2017.1420105, 2021.

Jin, H., Wu, Q., and Romanovsky, V.: Degrading permafrost and its impacts, Advances in Climate Change Research, 12, 10.1016/j.accre.2021.01.007, 2021.

Jin, H., Li, S., Cheng, G., Shaoling, W., and Li, X.: Permafrost and climatic change in China, Global and Planetary Change, 26, 387-404, https://doi.org/10.1016/S0921-8181(00)00051-5, 2000.

Jin, H., Yu, Q., Lü, L., Guo, D., He, R., Yu, S.-p., Sun, G., and Li, Y.: Degradation of permafrost in the Xing'anling Mountains, northeastern China, Permafrost and Periglacial Processes, 18, 245-258, 2007.

Li, X.-Y., Jin, H.-J., Wang, H.-W., Marchenko, S. S., Shan, W., Luo, D.-L., He, R.-X., Spektor, V., Huang, Y.-D., Li, X.-Y., and Jia, N.: Influences of forest fires on the permafrost environment: A review, Advances in Climate Change Research, 12, 48-65, https://doi.org/10.1016/j.accre.2021.01.001, 2021.

Li, X., Jin, H., He, R., Huang, Y., Wang, H., Luo, D., Jin, X., Lü, L., Wang, L., Li, W. h., Wei, C., Chang, X., Yang, S., and Yu, S.: Effects of forest fires on the permafrost environment in the northern Da Xing'anling (Hinggan) mountains, Northeast China, Permafrost and Periglacial Processes, 30, 163-177, https://doi.org/10.1002/ppp.2001, 2019.

Luo, D., Guo, D., Jin, H., Yang, S., Phillips, M. K., and Frey, B.: Ecological Impacts of Degrading permafrost, Frontiers in Earth Science, 10.3389/feart.2022.967530, 2022.

Luo, L., Ma, W., Zhuang, Y., Zhang, Y., Yi, S., Xu, J., Long, Y., Ma, D., and Zhang, Z.: The impacts of climate change and human activities on alpine vegetation and permafrost in the Qinghai-Tibet Engineering Corridor, Ecological Indicators, 93, 24-35, https://doi.org/10.1016/j.ecolind.2018.04.067, 2018.

Mu, C., Abbott, B. W., Norris, A. J., Mu, M., Fan, C., Chen, X., Jia, L., Yang, R., Zhang, T., Wang, K., Peng, X., Wu, Q., Guggenberger, G., and Wu, X.: The status and stability of permafrost carbon on the Tibetan Plateau, Earth-Science Reviews, 211, 103433, https://doi.org/10.1016/j.earscirev.2020.103433, 2020.

Ran, Y., Li, X., and Cheng, G.: Climate warming over the past half century has led to thermal degradation of permafrost on the Qinghai–Tibet Plateau, The Cryosphere, 12, 595-608, 10.5194/tc-12-595-2018, 2018.

Ran, Y., Li, X., Cheng, G., Che, J., Aalto, J., Karjalainen, O., Hjort, J., Luoto, M., Jin, H., Obu, J., Hori, M., Yu, Q., and Chang, X.: New high-resolution estimates of the permafrost thermal state and hydrothermal conditions over the Northern Hemisphere, Earth Syst. Sci. Data, 14, 865-884, 10.5194/essd-14-865-2022, 2022.

Romanovsky, V. E., Smith, S. L., and Christiansen, H. H.: Permafrost thermal state in the polar Northern Hemisphere during the international polar year 2007–2009: a synthesis, Permafrost and Periglacial Processes, 21, 106-116, https://doi.org/10.1002/ppp.689, 2010.

Schuur, E. A. G. and Mack, M. C.: Ecological Response to Permafrost Thaw and Consequences for Local and Global Ecosystem Services, Annual Review of Ecology, Evolution, and Systematics, 49, 279-301, 10.1146/annurev-ecolsys-121415-032349, 2018.

Schuur, E. A. G., McGuire, A. D., Schädel, C., Grosse, G., Harden, J. W., Hayes, D. J., Hugelius, G., Koven, C. D., Kuhry, P., Lawrence, D. M., Natali, S. M., Olefeldt, D., Romanovsky, V. E., Schaefer, K., Turetsky, M. R., Treat, C. C., and Vonk, J. E.: Climate change and the permafrost carbon feedback, Nature, 520, 171-179, 10.1038/nature14338, 2015.

Serban, R., Serban, M., He, R., Jin, H., Yan, L., Xinyu, L., Wang, X., and Li, G.: 46-Year (1973–2019) Permafrost Landscape Changes in the Hola Basin, Northeast China Using Machine Learning and Object-Oriented Classification, Remote Sensing, 13, 1910, 10.3390/rs13101910, 2021.

Shiklomanov, N., Streletskiy, D., and Nelson, F.: Northern Hemisphere Component of the Global Circumpolar Active Layer Monitoring (CALM) Program, 2012.

Shur, Y. and Jorgenson, M.: Patterns of Permafrost Formation and Degradation in Relation to Climate and Ecosystems, Permafrost and Periglacial Processes, 18, 7-19, 10.1002/ppp.582, 2007.

Sim, T. G., Swindles, G. T., Morris, P. J., Baird, A. J., Cooper, C. L., Gallego-Sala, A. V., Charman, D. J., Roland, T. P., Borken, W., Mullan, D. J., Aquino-López, M. A., and Gałka, M.: Divergent responses of permafrost peatlands to recent climate change, Environmental Research Letters, 16, 034001, 10.1088/1748-9326/abe00b, 2021.

Smith, S. L., Romanovsky, V. E., Lewkowicz, A. G., Burn, C. R., Allard, M., Clow, G. D., Yoshikawa, K., and Throop, J.: Thermal state of permafrost in North America: a contribution to the international polar year, Permafrost and Periglacial Processes, 21, 117-135, https://doi.org/10.1002/ppp.690, 2010.

Wei, Z., Jin, H., Zhang, J., Yu, S., Han, X., Ji, Y., He, R., and Chang, X.: Prediction of permafrost changes in Northeastern China under a changing climate, Science China Earth Sciences, 54, 924-935, 10.1007/s11430-010-4109-6, 2011.

Wu, T., Xie, C., Zhu, X., Chen, J., Wang, W., Li, R., Wen, A., Wang, D., Lou, P., Shang, C., La, Y., Wei, X., Ma, X., Qiao, Y., Wu, X., Pang, Q., and Hu, G.: Permafrost, active layer, and meteorological data (2010–2020) at the Mahan Mountain relict permafrost site of northeastern Qinghai–Tibet Plateau, Earth Syst. Sci. Data, 14, 1257-1269, 10.5194/essd-14-1257-2022, 2022.

Yang, J. M.: Genhe annals (1996-2005), Inner Mongolia Culture Press, Hailar,2007.

Yang, S. and Jin, H.: δ18O and δD records of inactive ice wedge in Yitulihe, Northeastern China and their paleoclimatic implications, Science China Earth Sciences, 54, 119-126, 10.1007/s11430-010-4029-5, 2011.

Zhang, G., Nan, Z., Wu, X., Ji, H., and Zhao, S.: The Role of Winter Warming in Permafrost Change Over the Qinghai-Tibet Plateau, Geophysical Research Letters, 46, 11261-11269, https://doi.org/10.1029/2019GL084292, 2019.

Zhang, T., Nelson, F., and Gruber, S.: Introduction to special section: Permafrost and Seasonally Frozen Ground Under a Changing Climate, Journal of Geophysical Research, 112, 10.1029/2007JF000821, 2007.

Zhang, Y., Cheng, G., Jin, H., Yang, D., Flerchinger, G., Chang, X., Wang, X., and Liang, J.: Influences of Topographic Shadows on the Thermal and Hydrological Processes in a Cold Region Mountainous Watershed in Northwest China, Journal of Advances in Modeling Earth Systems, 10, 10.1029/2017MS001264, 2018a.

Zhang, Y., Cheng, G., Jin, H., Yang, D., Flerchinger, G., Chang, X., Bense, V., Han, X., and Liang, J.: Influences of frozen ground and climate change on the hydrological processes in an alpine watershed: A case study in the upstream area of the Hei'he River, Northwest China, Permafrost and Periglacial Processes, 28, 420-432, 2017.

Zhang, Z.-Q., Wu, Q.-B., Hou, M.-T., Tai, B.-W., and An, Y.-K.: Permafrost change in Northeast China in the 1950s–2010s, Advances in Climate Change Research, 12, 18-28, https://doi.org/10.1016/j.accre.2021.01.006, 2021.

Zhang, Z., Wu, Q., Xun, X., Wang, B., and Wang, X.: Climate change and the distribution of frozen soil in 1980–2010 in northern northeast China, Quaternary International, 467, 230-241, https://doi.org/10.1016/j.quaint.2018.01.015, 2018b.

Zhao, L., Zou, D., Hu, G., Wu, T., Du, E., Liu, G., Xiao, Y., Li, R., Pang, Q., Qiao, Y., Wu, X., Sun, Z., Xing, Z., Sheng, Y., Zhao, Y., Shi, J., Xie, C., Wang, L., Wang, C., and Cheng, G.: A synthesis dataset of permafrost thermal state for the Qinghai–Tibet (Xizang) Plateau, China, Earth Syst. Sci. Data, 13, 4207-4218, 10.5194/essd-13-4207-2021, 2021.

Zou, D., Zhao, L., Sheng, Y., Chen, J., Hu, G., Wu, T., Wu, J., Xie, C., Wu, X., Pang, Q., Wang, W., Du, E., Li, W., Liu, G., Li, J., Qin, Y., Qiao, Y., Wang, Z., Shi, J., and Cheng, G.: A new map of permafrost distribution on the Tibetan Plateau, The Cryosphere, 11, 2527-2542, 10.5194/tc-11-2527-2017, 2017.

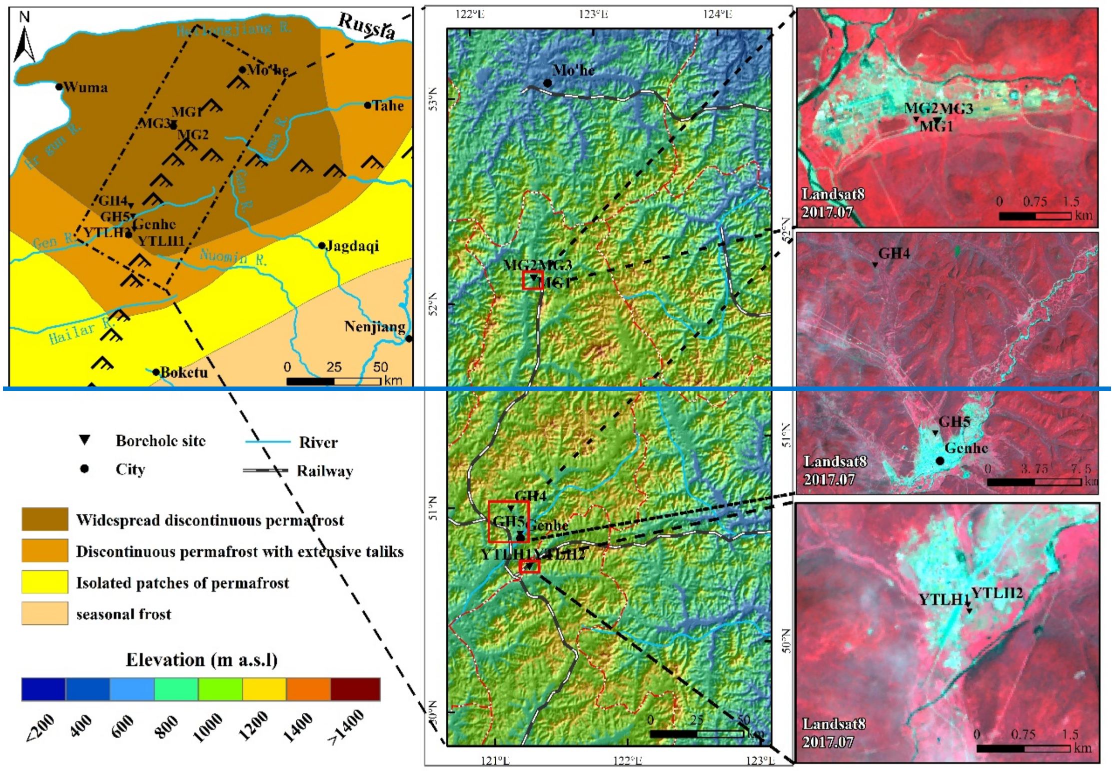

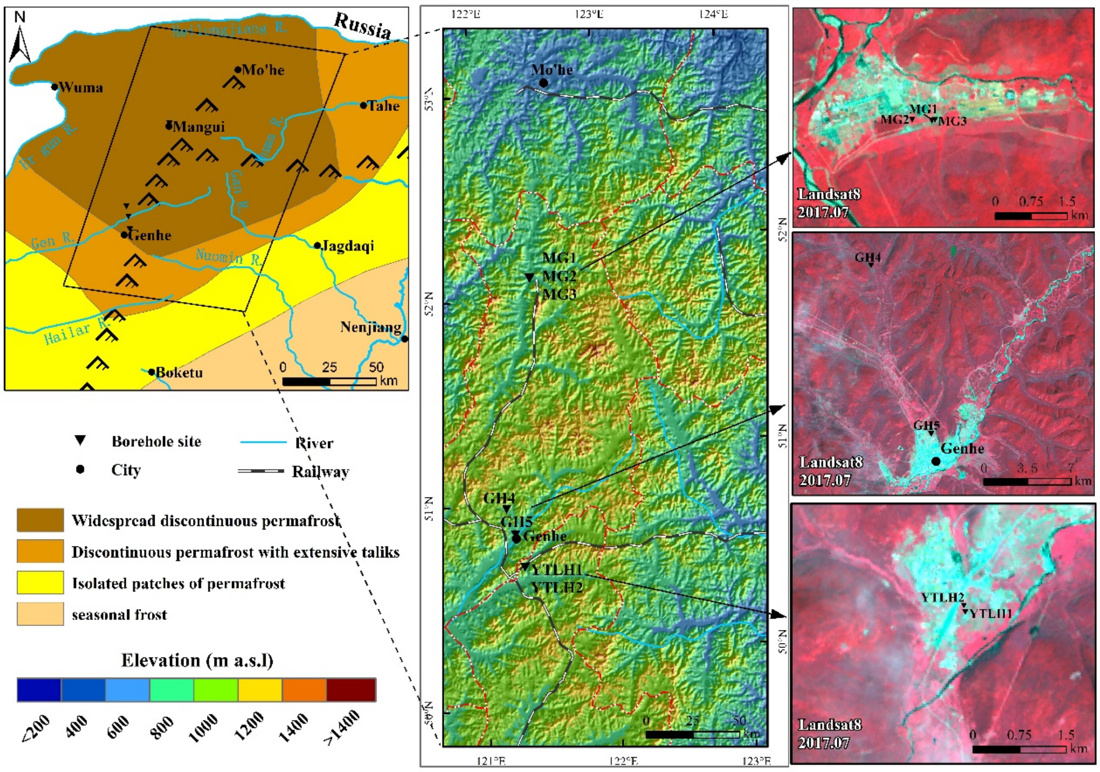

Figure 1. Location of the study area and the distribution of Mangui1 (MG1), Mangui2 (MG2), Mangui3 (MG3), Gen'he4 (GH4), Gen'he5 (GH5), Yituli'he1 (YTLH1) and Yituli'he2 (YTLH2) in the zones of frozen ground in the northern Da Xing"anling Mountains, Northeast China (The permafrost distribution is from Jin et al. (2007).)

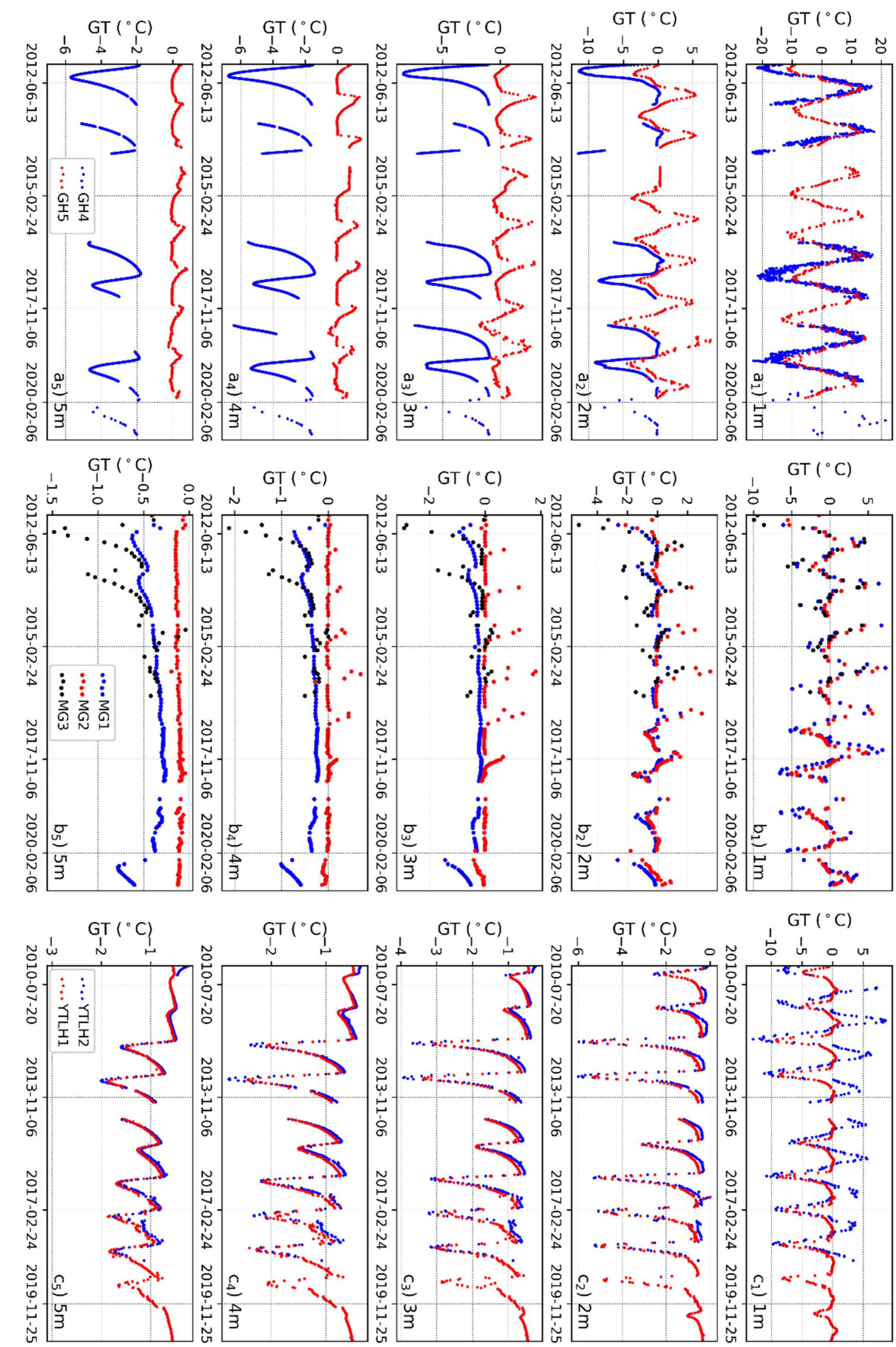

Figure 2. Variability of measured ground temperatures at depths of 1-5 m for Boreholes GH4 and GH5 (a)), MG1, MG2 and MG3 (b)), and YTLH1 and YTLH2 (c)).

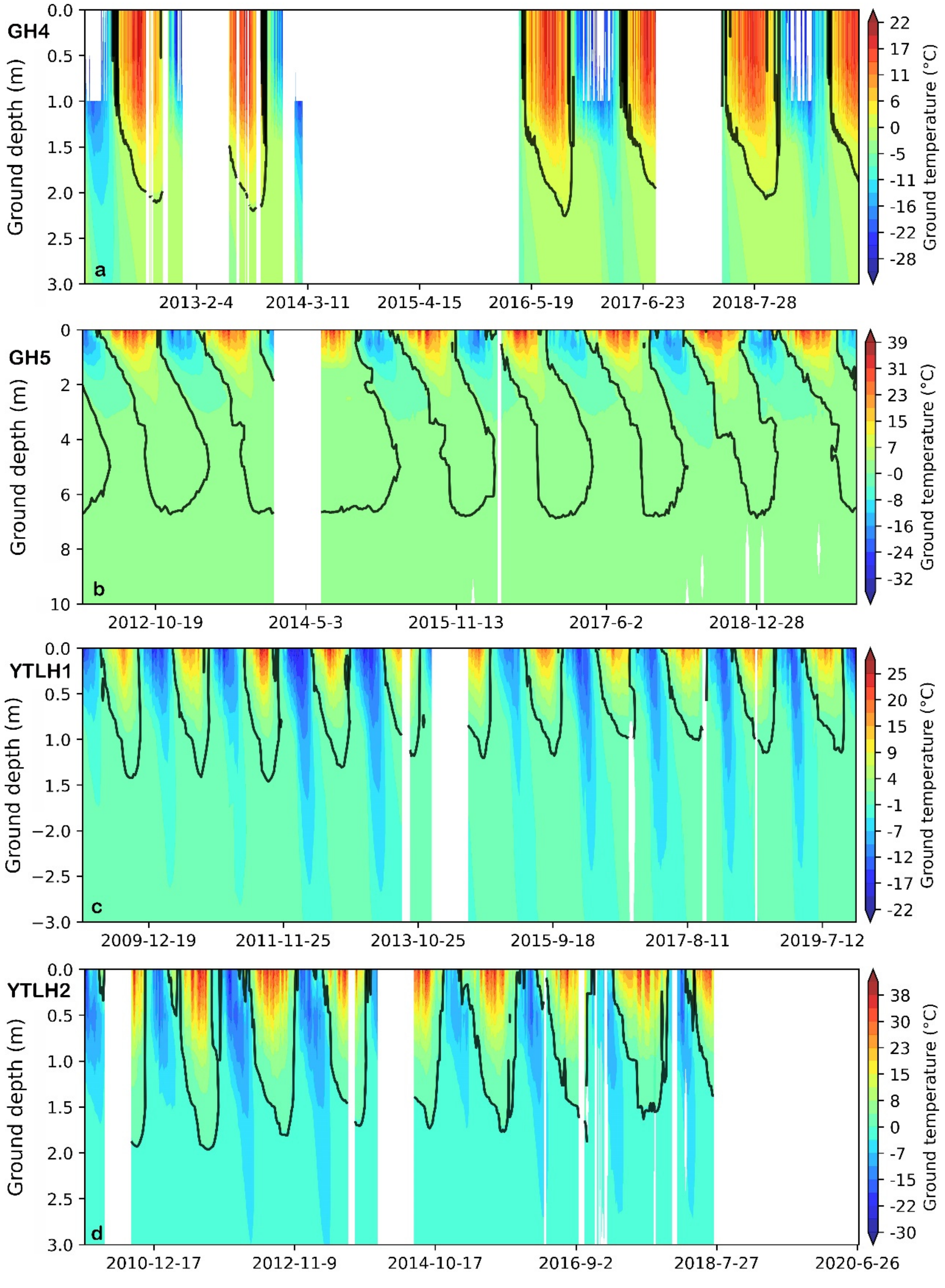

Figure 3 Variability of 0 °C isotherms (black curves) of ground temperature for Boreholes GH4 (a), GH5 (b), YTLH1 (c), and YTLH2 (d). The empty space indicates the period of missing data.

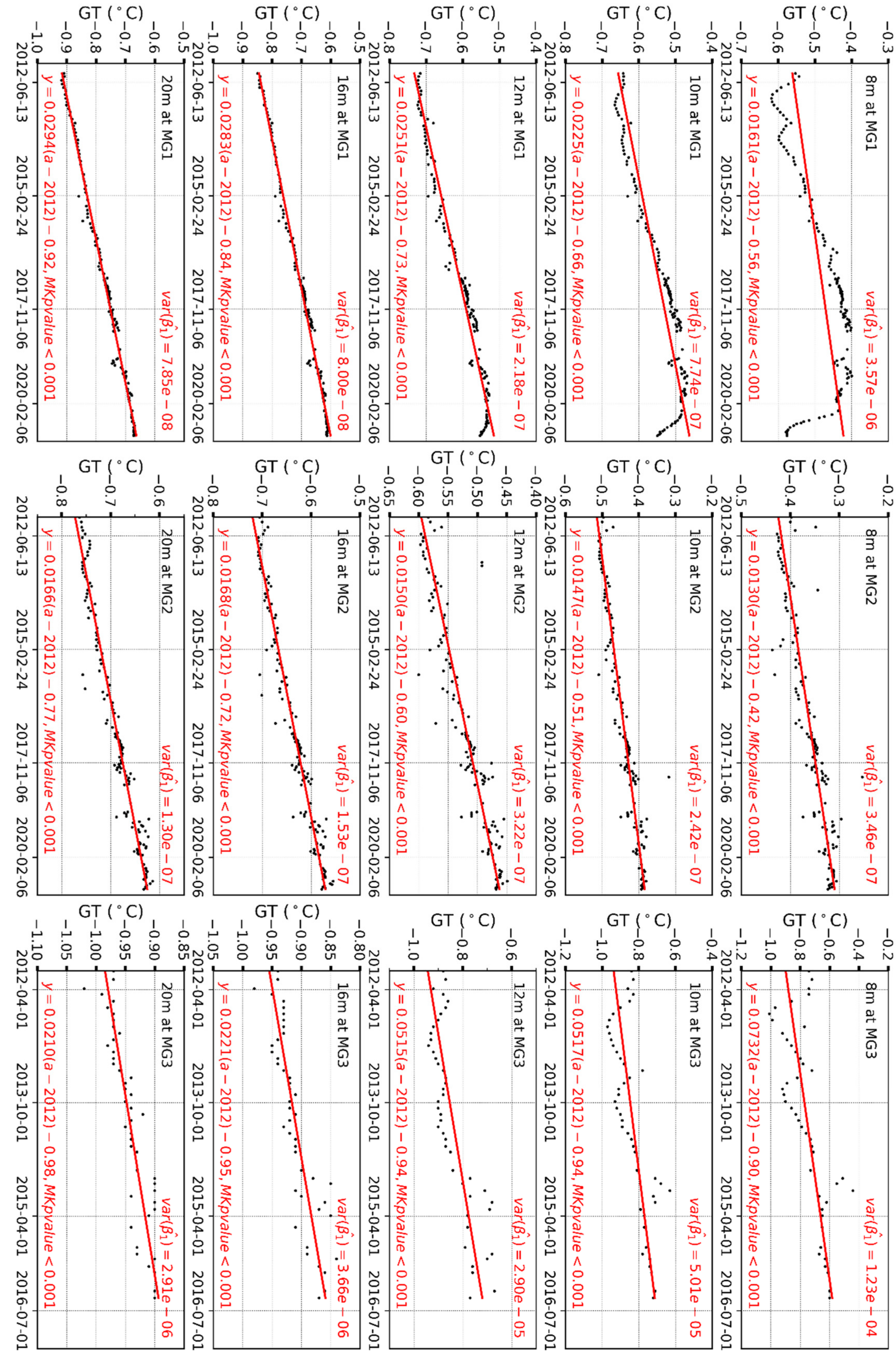

Figure 4. Variability of permafrost temperatures at depths of 8, 10, 12, 16 and 20 m in Boreholes MG1, MG2 and MG3 in Mangui, northern Da Xing'anling Mountains, Northeast China during 2012-2020. GT stands for ground temperature.

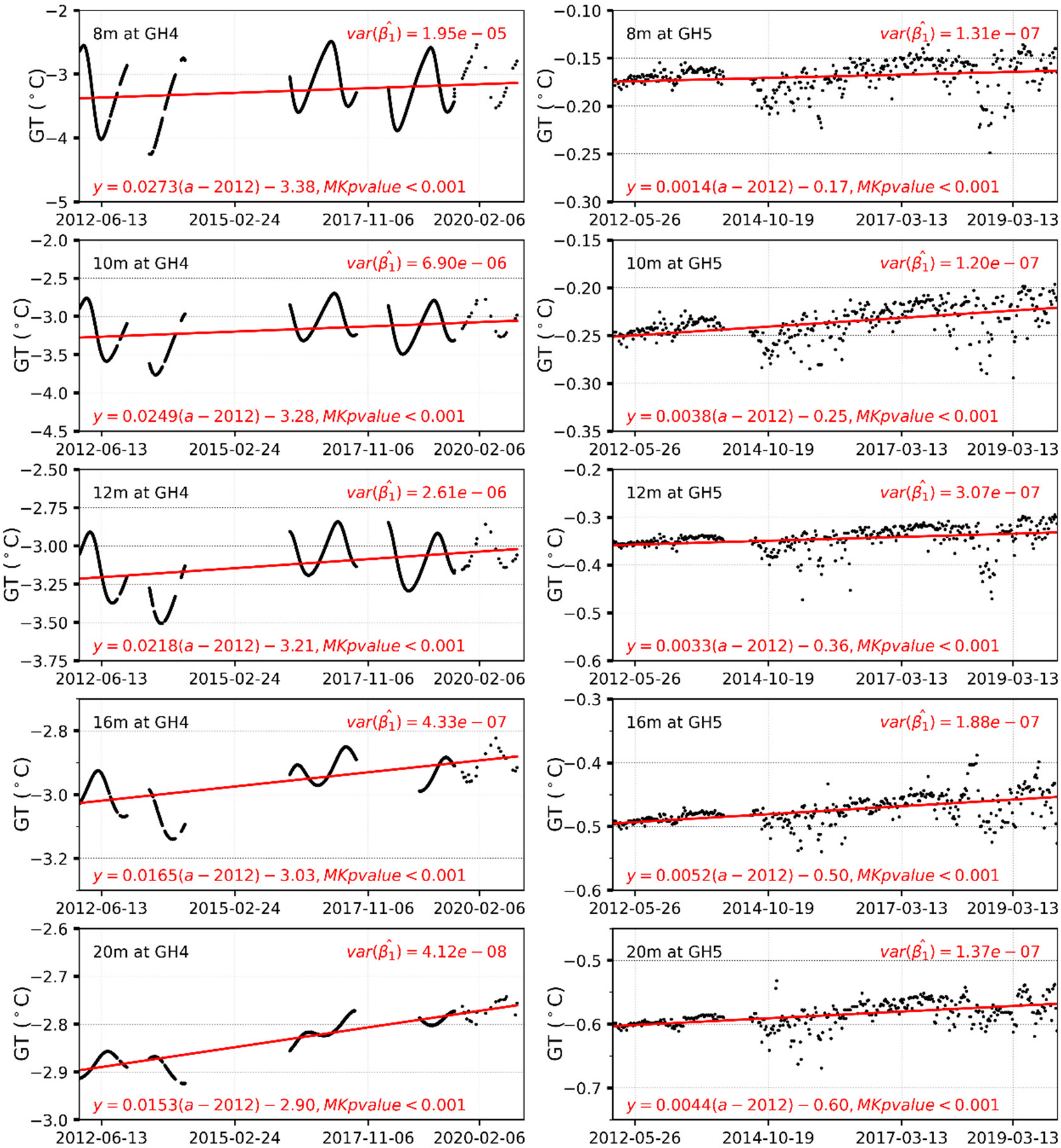

Figure 5. Variations in permafrost temperatures at depths of 8, 10, 12, 16 and 20 m in Boreholes GH4 and GH5 in Gen'he, northern Da Xing'anling Mountains, Northeast China during 2012-2020. GT stands for ground temperature.

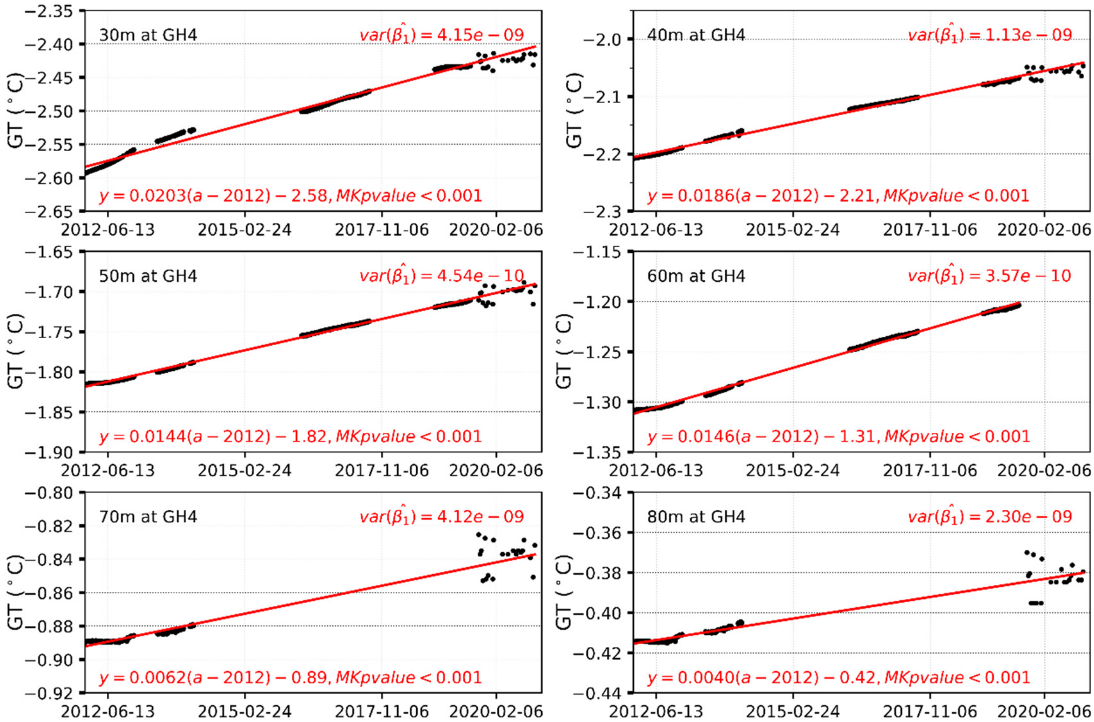

Figure 6. Variability of deep permafrost temperatures at depths of 30 – 80 m for Borehole GH4 in Gen'he, northern Da Xing'anling Mountains, Northeast China during 2012-2020. GT stands for ground temperature.

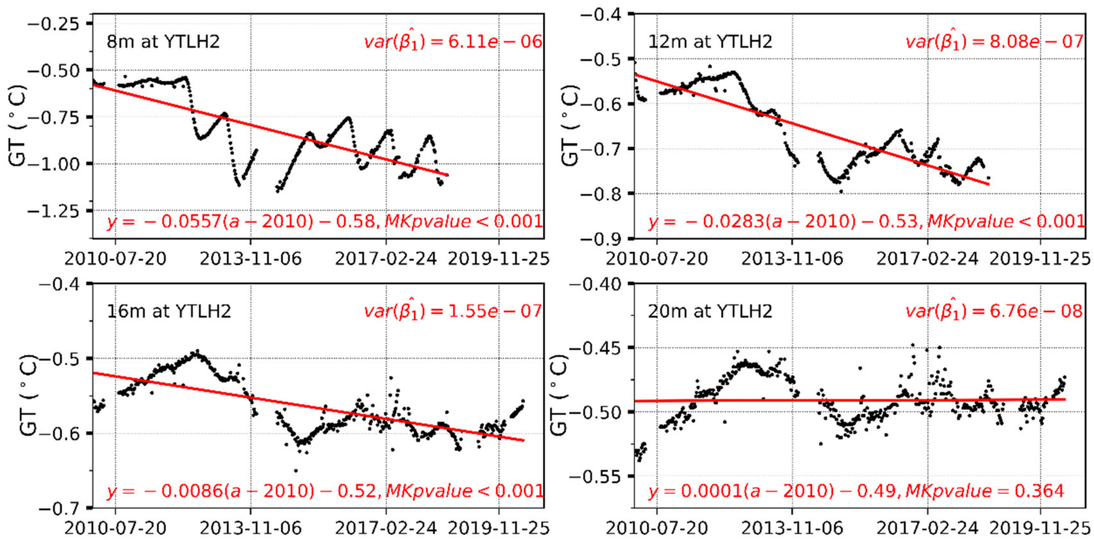

Figure 7. Variability of permafrost temperatures at depths of 8, 12, 16 and 20 m at Borehole YTLH2 in Yituli'he in northern Da Xing'anling Mountains, Northeast China during 2012-2020. GT stands for ground temperature.

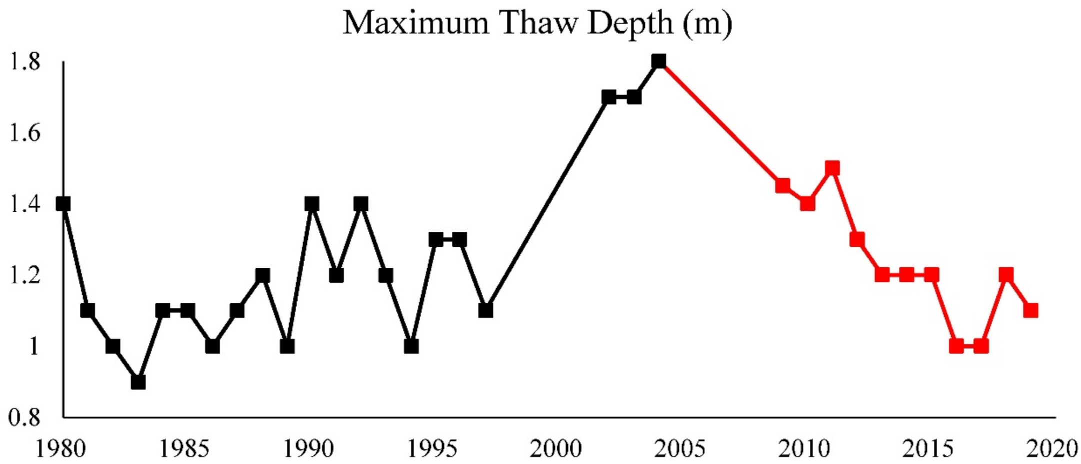

Figure 8. The maximum thaw depth (1980-2019) in Yituli'he on the northwestern flank of the northern Da Xing'anling Mountains in Northeast China (Black squares appeared in the paper from Jin et al. (2007), red ones are obtained in this observation. The two boreholes are 10 m from each other, with similar surface, hydrology and soil conditions.)

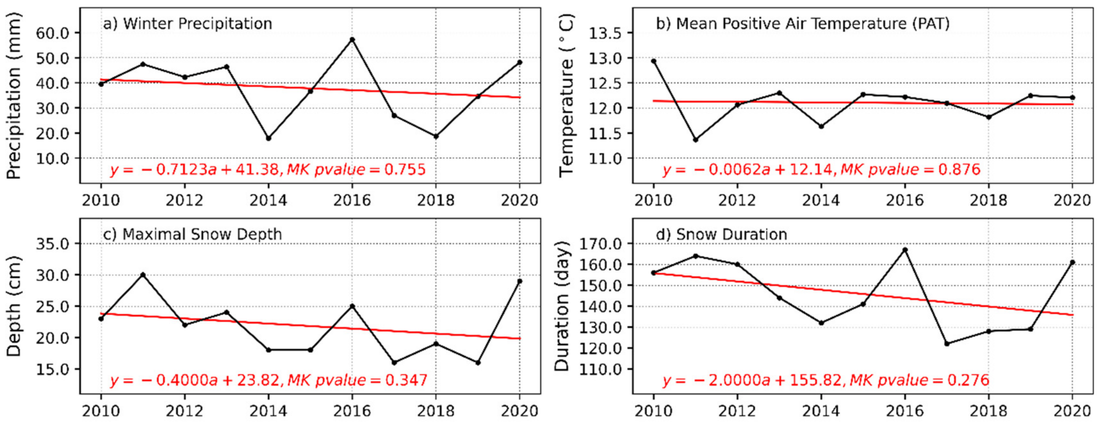

Figure 9. Climatic characteristics of Gen'he on the northwestern flank of the northern Da Xing'anling Mountains in Northeast China in the past ten years

Table 1. Characteristics and monitoring information of ground temperature boreholes in the northwestern part of Da Xing'anling Mountains, Northeastern China

Borehole No.	Lat. (°N)	Long. (°E)	Elev. (m a. s. l.)	Vegetation	Monitoring depths (m)	Time period	Monitoring frequency
MG1	52.037	122.069	633	*Betula fruticosa* shrubs		2012-2020	
MG2	52.036	122.075	642	*Carex tato* meadow	0.0, 1.0, 1.5, 2.0, 2.5, 3.0, 3.5, 4.0, 4.5, 5.0, 6.0, 7.0, 8.0, 9.0, 10.0, 11, 12, 13, 14, 15, 16, 17, 18, 19, 20	2012-2020	Monthly
MG3	52.036	122.076	639	Open courtyard		2012-2015	
GH4	50.932	121.502	811	*Betula fruticosa* *Larix gmelini* forest	0.0, 1.0, 1.5, 2.0, 2.5, 3.0, 3.5, 4.0, 4.5, 5.0, 6.0, 7.0, 8.0, 9.0, 10.0, 11, 12, 13, 14, 15, 16, 17, 18, 19, 20, 25, 30, 35, 40, 45, 50, 60, 70, 80	2012-2014, 2016-2017, 2019-2020	Hourly
GH5	50.799	121.530	728	*Carex tato* meadow	0.0, 1.0, 1.5, 2.0, 2.5, 3.0, 3.5, 4.0, 4.5, 5.0, 6.0, 7.0, 8.0, 9.0, 10.0, 11, 12, 13, 14, 15, 16, 17, 18, 19, 20	2012-2019	
YTLH1	50.629	121.549	721	*Carex tato* swamp	0.0, 0.1, 0.2, 0.5, 0.8, 1.0, 1.6, 2.0, 3.0, 4.0, 5.0, 6.0, 7.0, 8.15	2009-2019	Weekly
YTLH2	50.630	121.549	725	*Carex tato* swamp	0.0, 1.0, 1.5, 2.0, 2.5, 3.0, 3.5, 4.0, 4.5, 5.0, 6.0, 7.0, 8.0, 9.0, 10.0, 11, 12, 13, 14, 15, 16, 17, 18, 19, 20	2010-2017	

Table 2 ALT and average MAGTs of boreholes at larger depths in the northwestern Da Xing'anling Mountains, Northeast China

Borehole	ALT (m)	Average MAGT (°C)				
		8m	10m	13m	16m	20m
MG1	1.9-2.6	-0.48(ZAA)	-0.55	-0.63	-0.71	-0.77
MG2	4.3-4.8	-0.34(ZAA)	-0.44	-0.55	-0.63	-0.69
MG3	2.8-4.0	-0.75	-0.83	-0.87(ZAA)	-0.91	-0.94
GH4	2.0-2.2	-3.26	-3.17	-3.06	-2.96(ZAA)	-2.84
GH5	7.0	-0.17(ZAA)	-0.24	-0.39	-0.47	-0.59
YTLH2	1.5-2.0	-0.82	-0.74	-0.61(ZAA)	-0.56	-0.49